Mon. Not. R. Astron. Soc. **000**, 000–000 (0000) Printed 24 April 2007 (MN LATEX style file v2.2)

Hypervelocity stars and the environment of Sgr A*

Alberto Sesana[1,2], Francesco Haardt[1], & Piero Madau[3,4]
[1] *Dipartimento di Fisica e Matematica, Universitá dell'Insubria, Via Valleggio 11, 22100 Como, Italy*
[2] *School of Physics and Astornomy, University of Birmingham, Edgbaston, Birmingham, B15 2TT, UK*
[3] *Department of Astronomy & Astrophysics, University of California, Santa Cruz, CA 95064, USA*
[4] *Max-Planck-Institut fuer Astrophysik, Karl-Schwarzschild-Strasse 1, 85740 Garching bei Muenchen, Germany*

Received —

ABSTRACT
Hypervelocity stars (HVSs) are a natural consequence of the presence of a massive nuclear black hole (Sgr A*) in the Galactic Center. Here we use the Brown et al. sample of unbound and bound HVSs together with numerical simulations of the propagation of HVSs in the Milky Way halo to constrain three plausible ejection mechanisms: 1) the scattering of stars bound to Sgr A* by an inspiraling intermediate-mass black hole (IMBH); 2) the disruption of stellar binaries in the tidal field of Sgr A*; and 3) the two-body scattering of stars off a cluster of stellar-mass black holes orbiting Sgr A*. We compare the predicted radial and velocity distributions of HVSs with the limited-statistics dataset currently available, and show that the IMBH model appears to produce a spectrum of ejection velocities that is too flat. Future astrometric and deep wide-field surveys of HVSs should shed unambiguous light on the stellar ejection mechanism and probe the Milky Way potential on scales as large as 200 kpc.

Key words: black holes physics – Galaxy: center – Galaxy: kinematics and dynamics – stellar dynamics

1 INTRODUCTION

Hypervelocity stars (HVSs), i.e. stars moving with speeds sufficient to escape the gravitational field of the Milky Way (MW), were first recognized by Hills (1988) as an unavoidable byproduct of the presence of a massive black hole in the Galactic Center (GC). We now know of seven HVSs in the MW halo traveling with Galactic rest-frame velocities $v_{\rm RF}$ in the range between +400 and +750 $\rm km\,s^{-1}$ (Brown et al. 2005, 2006a,b; Hirsch et al. 2005; Edelmann et al. 2005). Most are probably B-type main sequence halo stars with galactocentric distances of 50-100 kpc, and have travel times from the GC consistent with their lifetimes. Only a close encounter with a relativistic potential well can accelerate a 3-4 $\rm M_\odot$ star to such extreme velocities, and at least three different ejection mechanisms from the dense stellar cusp around Sgr A*, the massive black hole in the GC, have been proposed:

(1) the scattering of stars bound to Sgr A* by an inspiraling intermediate-mass black hole ("IMBH model", Yu & Tremaine 2003; Levin 2006; Baumgardt et al. 2006; Sesana et al. 2006, 2007b).

(2) the tidal breakup of a tight stellar binary by Sgr A* (hereinafter the "TB model"). This interaction leads to the capture of one star and the high-speed ejection of its companion (Hills 1988; Yu & Tremaine 2003; Gualandris etal. 2005; Ginsburg & Loeb 2006; Bromley et al. 2006).

(3) the scattering of ambient stars by a cluster of stellar-mass black holes that have segregated around Sgr A* (O'Leary & Loeb 2006; Miralda-Escudé & Gould 2000; hereinafter the "BHC" model).

In theory, the observed frequency, spectral properties, and spatial and velocity distributions of HVSs should all shed light on the ejection mechanism and the stellar environment around Sgr A*. In practice, however, different scenarios can reproduce the inferred rate of removal from the GC simply by changing, within the observational constraints, the stellar mass function and/or the fraction of stellar binaries. Travel times estimates for the known HVSs are spread uniformly between 30 and 160 Myr, and there is as yet no evidence for a burst of HVSs from the GC (Brown et al. 2006a). Both models TB and BHC predict HVSs to be expelled isotropically at an approximately constant rate, while in model IMBH HVSs are ejected preferentially within the orbital plane of the black hole pair in a short burst lasting a few Myr (Levin 2006; Sesana et al. 2006, 2007a, 2007b). Even in the latter case, however, the observed HVS population would plausibly be produced by a series of IMBH inspiral events (at a rate that could be as high as 10^{-7} $\rm yr^{-1}$, see Portegies Zwart et al. 2006) with randomly oriented orbital planes. HVSs would then be distributed isotropically in the halo of the MW, and the imprint of a single burst on their spatial distribution would be hardly recognizable.

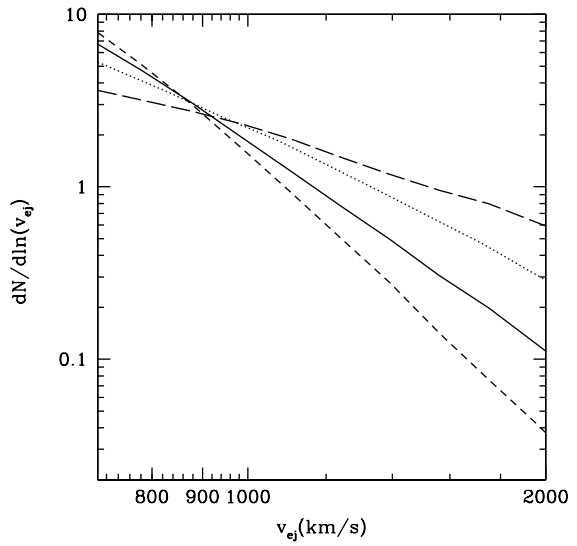

Figure 1. Distribution of ejection velocities of HVSs predicted by the three different mechanisms discussed in the text. *Short-dashed line*: model TBln. *Solid line*: model TBf. *Dotted line*: model BHC. *Long-dashed line*: model IMBH with $q = 1/729$ and $e = 0.9$. Models TBf and TBln assume a Salpeter initial mass function from 1 to 15 $M_\odot$. Only stars with ejection velocities $v_{\rm ej} > 700$ km s^{-1} will reach galactocentric distances $r > 10$ kpc. The average ejection velocities in the plotted range are 870, 930, 990, and 1160 km s^{-1} for models TBln, TBf, BHC, and IMBH, respecively. Curves are normalized so that the integral in $d\ln(v_{\rm ej})$ from $\ln(700/\,{\rm km\,s^{-1}})$ to infinity is unitary.

In this *Letter* we use numerical simulations of the propagation of HVSs in the Milky Way halo to compare the radial and velocity distributions predicted by the three models to the Brown et al. (2006a,b) sample of unbound and bound HVSs.

2 MODELS

HVSs are assumed to be ejected from the GC at a steady, arbitrary rate, and their velocities are obtained as follows:

(1) In model IMBH, HVSs are produced according to the velocity distribution of scattered stars found in scattering experiments (Sesana et al. 2006, 2007b). In Sesana et al. 2007b, we study the inspiral of an IMBH onto a MBH surrounded by a cusp of bound stars. Motivated by recent N-body simulations (Matsubayashi et al. 2007), we assume that the IMBH starts to eject stars when the total stellar mass inside the binary semimajor axis a is $\sim M_2$, the mass of the secondary. For Sgr A*, this translates into $a \simeq 0.03$ pc. We further assume a black hole binary mass ratio $q = 1/729$, an initial orbital eccentricity $e = 0.9$, and a stellar cusp (bound to Sgr A*) with density profile $\propto r^{-1.5}$. The IMBH is found to stall after loss–cone depletion at $a \sim 0.004$ pc. While the ejection rate depends on the values of q and e, neither the binary mass ratio nor its eccentricity have a large effect on the average ejection velocity (see also Fig. 6 of Sesana et al. 2006). We checked that either assuming $q = 1/243$ or $e = 0.1$, does not affect significantly the predicted velocity distribution. As the ejection velocity in a scattering event is a function of binary separation, the velocity distribution used here is averaged during the entire shrinking phase of the binary: the IMBH decays fast at large separations (where stars gain relatively little energy after an encounter), and ejects stars at higher and higher speeds as it approaches the hardening radius.

(2) For models TB invoking the tidal break-up of stellar binaries by a close encounter with Sgr A*, we use the results of the scattering experiments performed by Bromley et al. (2006). There, randomly oriented circular binaries are launched towards Sgr A* from a distance of several thousands AU at an initial approach speed of 250 km s^{-1}. The high-speed ejection of a binary member depends on the binary semi-major axis $a_{\rm bin}$, the closest approach distance between the binary and the hole, $R_{\rm min}$, and the masses of the three bodies. A Gaussian distribution of ejection speeds with 20% dispersion around the mean provides a reasonable characterization of the numerical results. We use this simple Gaussian model, assuming both a flat distribution in log $a_{\rm bin}$ (Heacox 1998, hereinafter TBf model), and a lognormal distribution in $a_{\rm bin}$ (Duquennoy & Major 1991, hereinafter TBln model). We randomly sample the closest approach distance $R_{\rm min}$ between 1 and 700 AU, and neglect any preference in the ejection of either members of the binary. Both binary member masses are generated according to a Salpeter initial mass function in the range 1-15 $M_\odot$.

(3) Finally, in model BHC, HVSs are generated from the conservative distribution of O'Leary & Loeb (2006, see their Figure 1), including encounters that results in physical star-black holes collisions. This is because the typical relative speed of the stars and the black holes is much larger than the surface escape velocity of the star: such encounters do not lead to coalescences and could also result in HVSs. All black holes have a mass of $m_{\rm BH} = 10$ km s^{-1}, are distributed isotropically, and follow a cuspy density profile with slope -2 (O'Leary & Loeb 2006). Compared to model IMBH in which a single scatterer slowly sinks inward, in model BHC many scattering centers are present at any given time around Sgr A*.

The distribution of stellar ejection velocities at infinite distance from Sgr A* (and in the absence of other gravitational sources) is shown in Figure 1 for the three scenarios discussed above, in the range $700 < v_{\rm ej} < 2000$ km s^{-1}. Mechanism IMBH clearly produces a more numerous population of high-speed events with $v_{\rm ej} > 900$ km s^{-1} compared to mechanisms TB and BHC. Note that, while in both models IMBH and BHC the ejection velocity is independent of stellar mass (for model BHC this is actually true only as long as the star is lighter than the scattering hole), in model TB the ejection velocity of the primary (secondary) component of a $m_1 > m_2$ stellar binary scales as $\sqrt{m_2}(m_1+m_2)^{-1/6}$ [$\sqrt{m_1}(m_1+m_2)^{-1/6}$] (Hills 1988).

3 SIMULATIONS

To generate a simulated catalog of HVSs in the MW halo, we sample the distributions in Figure 1 and integrate the orbits of ejected stars in a spherically symmetric potential using the fourth-order Runge-Kutta routine DOPRI5 (Dormand & Prince 1978). The fractional tolerated error, in position

and velocity of the star, is set to 10^{-12} per step, allowing a (fractional) total energy conservation accuracy $\sim 10^{-8}$.

The Galactic potential, the main-sequence lifetime of the stars $t_{\rm ms}$, and its ejection time relative to the present all determine the distribution of observable velocities as a function of galactocentric distance. For each star we randomly generate a time T since ejection between zero and the main sequence lifetime $t_{\rm ms}$, integrate its orbit for a time T, and then store its final distance and velocity. While stars ejected with lower speeds cannot reach large distances within a time $< t_{\rm ms}$ and will only populate the inner halo, the high-velocity tail can reach more distant regions of the MW within the stellar main-sequence lifetime (Bromley et al. 2006).

Stars are assumed to be injected in the GC at a constant rate according to a Salpeter IMF, $dN/dm_* \propto m_*^{-2.35}$. The scattering rate of stars having mass between m_* and $m_* + \Delta m_*$ is then given by $t_c^{-1}\,(dN/dm_*)\,\Delta m_*$, where t_c is the characteristic timescale between encounters. Since the orbits of stars of mass m_* are only followed for at most a main-sequence timescale $t_{\rm ms}(m_*)$, we must normalize the total number of events according to

$$\Delta N(m_*) = \frac{t_{\rm ms}(m_*)}{t_c}\,\frac{dN}{dm_*}\,\Delta m_*. \qquad (1)$$

The number of stars ejected in the same mass interval is then $\Delta N(m_*)F(m_*)$, where the dimensionless function $F(m_*)$ takes into account the mass dependence of the ejection mechanism (as in model TB the ejection probability is larger for low-mass binaries, Hills 1988). Note that, in all models, the stellar lifetime introduces an explicit dependence on stellar mass in the spatial distribution of observable HVSs, since more massive stars need higher ejection speeds to reach large galactocentric distances.

To bracket the uncertainties in the MW potential, we have used 5 different models for the mass distribution in the Galaxy. One is the single-component default model used by Bromley et al. 2006 (hereinafter potential Bdef), a cored power-law

$$\rho(r) = \rho_0 / \left[1 + (r/r_c)^2\right], \qquad (2)$$

where $\rho_0 = 1.27 \times 10^4\ {\rm M}_\odot/{\rm pc}^3$ is the central density, and the core radius is $r_c = 8$ pc. The other four are multi-component models, formed by a power-law stellar bulge, an exponential disk, and an NFW (Navarro, Frank & White 1997) dark matter halo. In model WDa, the disk and halo are chosen according to model MWa of Widrow & Dubinsky (2005), and the bulge mass is set to $1.4 \times 10^{10}\,{\rm M}_\odot$. In models DB2d and DB4d, disk and halo are chosen according to models 2d and 4d of Dehnen & Binney (1998), and the bulge mass is $0.8 \times 10^{10}\,{\rm M}_\odot$. Finally, a variant of model WDa is constructed where the disk has the same mass but a smaller scale length $R_d = 2$ kpc, and the halo has a larger scale length (19 kpc) and is more massive ($M_{h,100} = 9.4 \times 10^{11}\ {\rm M}_\odot$). Such model, termed "Deep", is characterized by a large local escape speed. For simplicity, in all models the bulge is spherically symmetric and the disk mass is added as a spherical component to the bulge and halo. The disk contribution to the potential is significant only in models DB2d and Deep, and only in the inner 3-8 kpc. Table 1 list several observable quantities for the five assumed MW mass distributions. The potential gets shallower from top to bottom, with extreme models Deep and DB4d bracketing the range allowed by the observations.

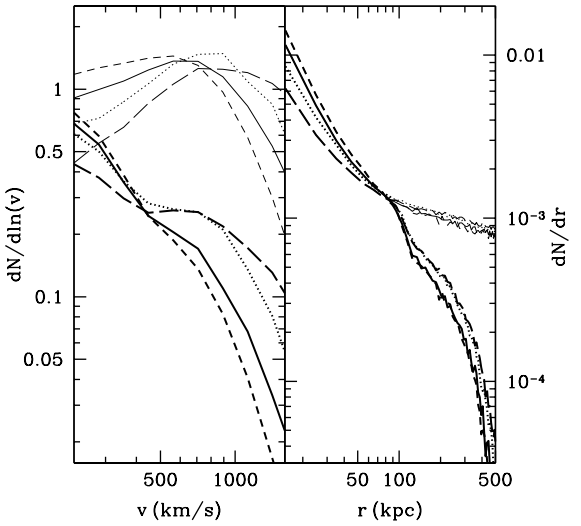

Figure 2. Normalized distribution of observable velocities $v > 200\ {\rm km\,s^{-1}}$ and galactocentric distances $r > 10$ kpc of stars ejected from the GC. Linestyles as in Fig. 1. All models assume a Salpeter initial mass function in the range $1-15\,{\rm M}_\odot$, and the MW potential WDa. *Thin lines:* all stars. *Thick lines:* stars brighter than $m_V = 24.5$ (see § 4 for details). *Left panel*: velocity distribution. *Right panel*: radial distribution.

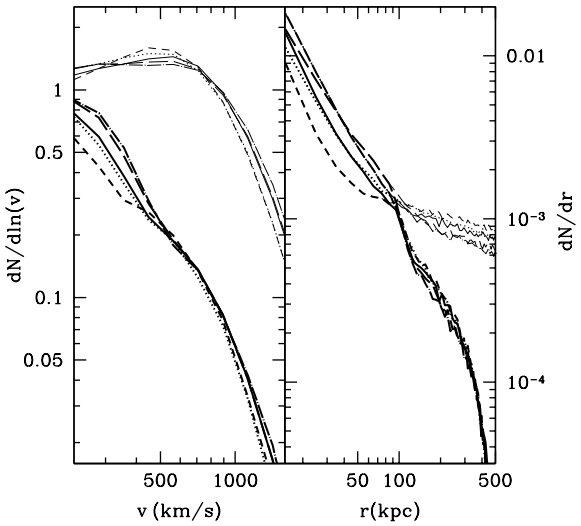

Figure 3. Same as Fig. 2, but for the TBln ejection mechanism and different MW potentials: Deep (*dot-dashed lines*), Bdef (*long-dashed lines*), WDa (*solid lines*), DB2d (*dotted lines*) and DB4d (*short-dashed lines*).

Combining the different ejection mechanisms with the MW gravitational potentials yields a total of twenty different models for the distributions observable speeds and distances of HVSs. These are shown in Figures 2 and 3 for stars with $v > 200\ {\rm km\,s^{-1}}$ and $r > 10$ kpc. The velocity distribution shows a broad peak for $v \sim 500 - 800\ {\rm km\,s^{-1}}$, and differ-

	$M_{0.01}$	M_{100}	$V_{c,8}$	A	B	$V_{\rm esc}$	$V_{\rm esc,8}$
Deep	3.46	10.0	207	15.0	-11.0	978	630
Bdef	2.93	10.2	210	13.2	-13.2	929	585
WDa	3.45	6.7	229	14.8	-13.9	899	550
DB2d	2.98	6.3	206	14.0	-11.9	824	515
DB4d	2.97	4.0	217	14.4	-13.0	791	455

Table 1. The five different models of MW mass distribution discussed in the text. The quantities $M_{0.01}, M_{100}, V_{c,8}, A, B, V_{\rm esc}$, and $V_{\rm esc,8}$ are, respectively, the mass enclosed in 10 pc in units of $10^7\,{\rm M}_\odot$, the mass enclosed in 100 kpc in units of $10^{11}\,{\rm M}_\odot$, the circular velocity at 8 kpc in ${\rm km\,s^{-1}}$, the Oort constants, the escape velocity from Sgr A* in ${\rm km\,s^{-1}}$; the escape velocity at 8 kpc in ${\rm km\,s^{-1}}$.

ent ejection scenarios are clearly recognizable. For the same ejection mechanism, the effect of the different MW potentials is relatively weak (Fig. 3, left panel). The distribution of galactocentric distances is instead quite sensitive to both the ejection and the potential model, particularly for stars within 100 kpc of the GC. Note that a steady rate of ejection of HVSs from the GC would result in a flat dN/dr curve. The excess at $r \lesssim 50$ kpc is due to the many low-mass stars that are scattered into the halo on bound orbits.

4 COMPARISON WITH THE OBSERVATIONS

We compare our predicted observable distributions to the Brown et al. sample of HVSs. The sample comprises 5 stars with $v_{\rm RF} > +400\ {\rm km\,s^{-1}}$ and $r > 50$ kpc (the unbound genuine HVSs of Brown et al. 2006a), as well as 7 candidate HVSs with $+275 < v_{\rm RF} < +450\ {\rm km\,s^{-1}}$ and distances greater than 10 kpc (the new class of possible "bound HVSs" recently advocated by Brown et al. 2007). The combined survey selects B stars with $3\,{\rm M}_\odot < m_* < 4\,{\rm M}_\odot$ down to a faint magnitude limit of $m_V = 19.5$, and is 100 % complete across the high declination region of the Sloan Digital Sky Survey, Data Release 4. Completeness is to a depth of 10-120 kpc (10-90 kpc) for 4 (3) ${\rm M}_\odot$ stars. As the actual ejection rates of the different mechanisms depend upon the poorly constrained properties of the stellar population in the GC (and, for model IMBH, on the eccentricity and mass of the secondary black hole), we only consider here normalized distribution of velocities and distances. Model predictions are shown only for stars in the mass range 3 to 4 ${\rm M}_\odot$. The theoretical distributions of observable velocities at all distances > 10 kpc are plotted in Figure 4 against the observations. Model IMBH clearly produces a long tail of HVSs with $v > 1500\ {\rm km\,s^{-1}}$, and a mean velocity of ejected stars that is larger compared to other mechanisms. For example, the mean velocity of HVSs in a WDa potential is $(594, 429, 403, 343)\ {\rm km\,s^{-1}}$ for models IMBH, BHC, TBf, and TBln, respectively. The TBf and BHC scenarios predict similar distributions, with BHC slightly shifted towards higher velocities. Predictions for the tidal break-up models are somewhat sensitive to the semimajor axis distribution of stellar binaries. In model TBln close binaries are rarer compared to model TBf, and the high-velocity tail of the velocity distribution is less pronounced. Table 2 shows the results of the two-dimensional, two-sample Kolmogorov-Smirnov (KS) test (Press et al. 1992) applied to the observed bivariate distance/velocity distribution of HVSs. This is compared to synthetic data sets of the same size drawn from the theoretical distributions of HVSs with masses of 3-4 ${\rm M}_\odot$, distances $r > 10$ kpc, and velocities $v > +275\ {\rm km\,s^{-1}}$. [1] Statistically, there is no difference between data and simulations only in the case of model TBln in shallow potentials (DB2d and DB4d). Within the limited-statistics dataset currently available, model IMBH appears to be disfavoured.

Slowly-moving, short-lived massive stars can only populate the inner halo, and ejection mechanisms like TBln and TBf that produce many low-speed events will generate a spatial distribution with an "excess" of stars within ∼50 kpc of the GC. Figure 5 shows the mean observable speed of 3-4 ${\rm M}_\odot$ HVSs as a function of galactocentric distance.

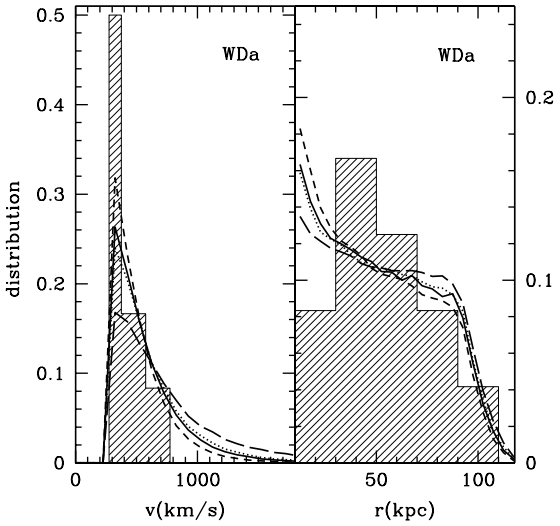

Figure 4. Theoretical distributions of observable speeds (*left panel*) and galactocentric distances (*right panel*) of ejected stars in the WDa potential. Model predictions are shown for stars in the mass range 3-4 ${\rm M}_\odot$, distances $r > 10$ kpc, and velocities $v > +275\ {\rm km\,s^{-1}}$. Linestyles as in Fig. 1. The shaded histogram represents one possible realization from the Brown et al. (2007) sample of bound and unbound HVSs.

	TBln	TBf	BHC	IMBH
Deep	0.151	0.085	0.057	0.007
Bdef	0.150	0.105	0.060	0.010
WDa	0.165	0.110	0.070	0.008
DB2d	0.215	0.149	0.127	0.014
DB4d	0.209	0.147	0.127	0.015

Table 2. Two-dimensional, two-sample Kolmogorov-Smirnov test significance for the observed distance-velocity distribution of HVSs compared to our twenty different (ejection mechanisms/MW potential) models.

[1] Note that the analysis of Brown et al. (2007) yields a statistically significant excess of 7 out of 11 observed "bound" stars, allowing for a total of 330 random realizations of the real data.

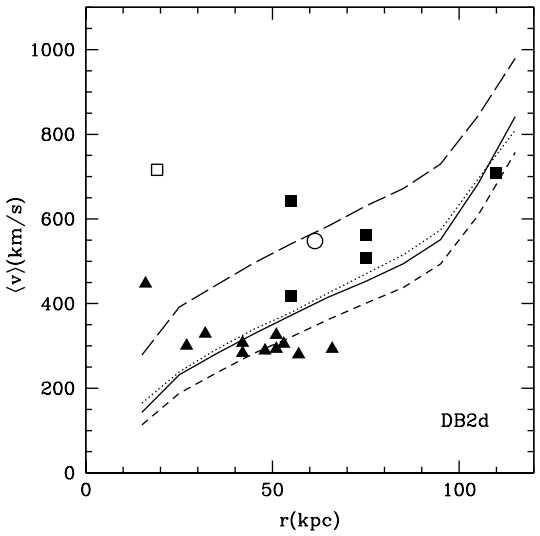

Figure 5. Mean observable speed of ejected stars in the mass range 3-4 $M_\odot$, as a function of galactocentric distance, for a DB2d MW potential. Linestyles as in Fig. 1. *Filled squares*: the 5 genuine unbound HVSs of the Brown et al. (2006a) sample. *Filled triangles*: the 11 stars with $+275 < v_{\rm RF} < +450$ km s^{-1} of the Brown et al. sample. About 7 of them are candidate bound HVSs. *Open square*: the HVS from Hirsch et al. (2005). *Open circle*: the HVS from Edelmann et al. (2005).

This is an increasing function of r because of stellar lifetime effects. Model IMBH appears to produce an excess of extremely fast-moving stars compared to the observations. We stress that this result does not depend on the values assumed for q and e. In particular, we tested that increasing q and/or decreasing e do not suppress the high velocity tail.

5 DISCUSSION

HVSs are in principle a powerful probe of the MW dark matter halo. Table 2 shows that, for any given ejection mechanism, the currently available statistics is far too low to constrain the MW potential (cf. Bromley et al. 2006). The situation will change dramatically with future astrometric (Gnedin et al. 2005) and deep wide-field surveys. For illustrative purposes, we focus here on *Large Synoptic Survey Telescope* (*LSST*, Claver et al. 2004). The *LSST* is being designed to survey an area of 20,000 deg^2 with 15 secs pointings, down to a limiting magnitude of $m_V = 24.5$. To assess the impact of the *LSST* on studies of HVSs, we first assign a survey volume to the theoretical models discussed in the previous sections and use the Brown et al. sample to estimate the expected number of HVSs detectable by the *LSST*. Assuming that the model distributions do indeed describe the parent population of HVSs, we then extract randomly from each of them a mock catalogue of HVSs. We then apply K-S statistics to quantify the ability of the *LSST* to distinguish between different scenarios.

As an illustrative example, we show in Figure 2 the distribution of observable speeds and distances predicted by the different ejection scenarios, for all $v > +200$ km s^{-1} and $r > 10$ kpc HVSs in the *LSST* survey volume. At a magnitude limit of $m_V = 24.5$, a 1 $M_\odot$ star can be detected at a distance of $\lesssim 100$ kpc, and the distance distributions drop rapidly at larger distances. Assuming a Salpeter initial mass function and ejection model TBln in a DB2d potential, we estimate that the *LSST* should detect $\sim 2500 \pm 800$ HVSs with $v > +275$ km s^{-1}, in the mass range $1 - 15$ $M_\odot$. We find that the detection of $\gtrsim 100$ HVSs may be enough to identify unambiguously the ejection model *and* the Galactic potential.

ACKNOWLEDGMENTS

Support to this work was provided by NASA grants NAG5-11513, NNG04GK85G, and by the Alexander von Humboldt Foundation (P.M.).

REFERENCES

Baumgardt H., Gualandris A. & Portegies Zwart S., 2006, MNRAS, 372, 174
Bromley B. C., Kenyon S. J., Geller M. J., Barcikowski E., Brown W. R. & Kurtz M. J., 2006, ApJ, in press (astro-ph/0608159)
Brown W. R., Geller M. J., Kenyon S. J. & Kurtz M. J., 2005, ApJ, 622, L33
———, 2006a, ApJ, 640, L35
———, 2006b, ApJ, 647, 303
Brown W. R., Geller M. J., Kenyon S. J., Kurtz M. J. & Bromley B. C., 2007, ApJ, in press (astro-ph/0701600)
Claver C. F. et al., 2004, Ground-based Telescopes, proceedings of the SPIE, 5489, 705
Dehnen W. & Binney J., 1998, MNRAS, 294, 429
Dormand J. R. & Prince P. J., 1978, CeMec, 18, 223
Duquennoy A. & Mayor M., 1991, A&A, 248, 485
Edelmann H., Napiwotzki R., Heber U., Christlieb N. & Reimers D., 2005, ApJ, 634, L181
Ginsburg I. & Loeb A., 2006, MNRAS, 368, 221
Gnedin O. Y., Gould A., Miralda-Escudé J. & Zentner A. R., 2005, ApJ, 634, 344
Gualandris A., Portegies Zwart S. & Sipior M. S., 2005, MNRAS, 363, 223
Heacox W. D., 1998, AJ, 115, 325
Hills J. G., 1988, Natur, 331, 687
Hirsch H. A., Heber U., O'Toole S. J. & Bresolin F., 2005, A&A, 444, L61
Levin Y., 2006, ApJ, 653, 1203
Matsubayashi T., Makino J. & Ebisuzaki T., 2007, ApJ, 656, 879
Miralda-Escudè J. & Gould A., 2000, ApJ, 545, 847
Navarro J. F., Frenk C. S. & White S. D. M., 1997, ApJ, 490, 493
O'Leary R. M. & Loeb A., 2006, MNRAS, submitted (astro-ph/0609046)
Portegies Zwart S. F., Baumgardt H., McMillan S. L. W., Makino J., Hut P. & Ebisuzaki T., 2006, ApJ, 641, 319
Press W. H., Teukolsky S. A., Vetterling W. T. & Flannery B. P., 1992, Numerical recipes in FORTRAN. The art of scientific computing, Cambridge: University Press
Sesana A., Haardt F. & Madau P., 2006, ApJ, 651, 392
———, 2007a, ApJ, in press (astro-ph/0612265)
———, 2007b, in preparation
Widrow L. M. & Dubinski J., 2005, ApJ, 631, 838
Yu Q. & Tremaine S., 2003, ApJ, 599, 1129